Available online at www.sciencedirect.com

ScienceDirect

journal homepage: www.intl.elsevierhealth.com/journals/dema

Novel dental resin composites containing LiAl-F layered double hydroxide (LDH) filler: Fluoride release/recharge, mechanical properties, color change, and cytotoxicity

Liang Wei Su[a], *Dan Jae Lin*[b,c,d,e,*], *Jun Yen Uan*[a,f,**]

[a] *Department of Materials Science and Engineering, National Chung Hsing University, Taiwan, ROC*
[b] *Department of Dental Hygiene, China Medical University, Taichung, Taiwan, ROC*
[c] *School of Dentistry, College of Dentistry, China Medical University, Taichung, Taiwan, ROC*
[d] *Graduate Institute of Biomedical Science, College of Medicine, China Medical University, Taichung, Taiwan, ROC*
[e] *Biomaterials Translational Research Center, China Medical University Hospital, Taichung, Taiwan, ROC*
[f] *Innovation and Development Center of Sustainable Agriculture (IDCSA), National Chung Hsing University, Taiwan, ROC*

ARTICLE INFO

Article history:
Received 22 September 2018
Received in revised form
26 January 2019
Accepted 4 February 2019

Keywords:
Restorations
Resin composites
Fluoride release
Recharge capability
Layered double hydroxide

ABSTRACT

Objectives. A novel LiAl-F layered double hydroxide (LDH) with a beneficial anions-exchangeable feature was developed for use as a fluoride reservoir. This study aims to investigate the fluoride release/ recharge capability of an LDH-contained dental resin composite and their effects on physical and biological properties.

Methods. 3% and 5% of LDH (R3, R5), wet-milled micro-scale LDH (R3W, R5W), or dry-milled nano-scale LDH (R3D, R5D) were added to a micro-hybrid flowable resin composite (RX). A commercial dental compomer (CC) was selected for comparison. An ion selective electrode recorded the daily fluoride release for 90 days (Daily fluoride recharging from 30th to 60th day). The flexural tests were performed according to ISO 4049. Also, the surface microhardness, color changes (L^*, a^*, b^*), Al^{3+}/Li^+ ion leaching, and cytotoxicity were evaluated.

Results. The LDH-contained resin composites show significantly increased fluoride release and recharge capability. Among them, R3 and R5 have more stable and long-term fluoride release than R3W, R5W, R3D, R5D, and CC. The LDH filler did not induce cytotoxicity, although few amounts of Al^{3+}/Li^+ ions were detected on the first day. The LDH filler did not alter the flexural strength of RX, and the microhardness (R3, R5, R3D, and R5D) was significantly higher than the CC group ($P < 0.01$). The LDH filler slightly increased the color of the composite in red (a^* values) and yellow (b^* values).

Significance. The LiAl-F LDH can be a fluoride reservoir filler for dental resin composites that increases the anti-caries ability.

* *Corresponding author at*: Department of Dental Hygiene, China Medical University, Taichung, Taiwan, ROC
** *Corresponding author at*: Department of Materials Science and Engineering, National Chung Hsing University, Taiwan, ROC
E-mail addresses: djlin@mail.cmu.edu.tw (D.J. Lin), jyuan@drogon.nchu.edu.tw (J. Yen Uan).

https://doi.org/10.1016/j.dental.2019.02.002
0109-5641/

1. Introduction

Dental caries is one of the most common oral prevalent diseases of people worldwide. According to statistics from the World Health Organization (WHO), dental caries affects 60–90% of school children and the vast majority of adults in most industrialized countries [1]. In 1996, Kaste et al. [2] who integrated previous surveys of dental caries, demonstrating that the occlusal surface was the most frequent site affected. The vulnerability of occlusal pits and fissures to dental decay is a problem which has prompted the development of pit and fissure sealants. In 1955, Buonocore's classic study [3], the introduction of the first dental pit and fissure sealant, was considered as the start of a major revolution in the clinical practice of dentistry. Caries reductions, however, were observed from 1970 [4]. The decline of caries resulted from the universal use of fluoride-containing products such as water fluoridation [4], fluoride toothpaste [5], fluoride mouthrinses [6,7], and others. Numerous studies have demonstrated that the ability of fluoride to prevent and arrest caries has three principal topical mechanisms of actions, inhibiting bacterial metabolism, inhibiting demineralization and enhancing remineralization [8–12]. With the increasing evidence of fluoride for caries prevention, several studies have looked at the benefits of adding fluoride to a sealant. In 1971, Lee et al. [13], adding Na_2PO_3F into dental sealant as an anticariogenic system, showing that persistent released fluoride on the enamel surface could maintain for an extended period of 24 h to 30 days and it was effective in reducing the incidence of carious lesions in molar teeth in vivo study. In 1985, el-Mehdawi et al. [14], added NaF into fissure sealant, their results indicated that higher concentration of fluoride was obtained from increasing the proportion NaF added. In 1971, a glass-ionomer cement (GIC) fissure sealant was developed by Wilson and Kent [15]. The GIC, a translucent cement for dental restoration, has become popular due to several advantages such as fluoride release, biocompatibility, modulus of elasticity, the coefficient of thermal expansion and adhesion to dentin [16–18]. However, conventional GICs have limitations as restorative materials, which are related to their susceptibility to dehydration and low occlusal wear resistance [2,19]. Combinations of GICs and composite resins (resin-modified GICs (RMGI) or polyacid-modified composites (compomer)) have been developed to obtain an adequate mechanical strength [20]. Even though RMGIs are reported to show better mechanical properties than the conventional GICs, their intrinsic toxicity exists due to elements leaching such as Al^{3+} [21–23]. Besides, numerous resin-based composites containing fluoride salts have been used in the clinical application. However, most of these resin composites presented a low fluoride releasing capacity and unknown fluoride recharging capacity [24]. Several investigators have shown that fluoride in the solution surrounding the carbonated apatite crystals is much more effective at inhibiting demineralization and enhancing remineralization [12,25,26]. The above studies indicate a long term fluoride recharging ability which could give sustainability and stability in fluoride-releasing restorative materials.

In recent years, much attention has focused on the development of composites prepared by dispersing layered fillers in a polymeric matrix to obtain optimized properties. In particular, layered double hydroxide (LDHs), or hydrotalcite-like compounds, are well-known layered material that has attracted increasing attention in recent years. LDHs have great application potential and been already used as catalysts, catalyst support, adsorbent or drug carrier due to large interlayer spaces and exchangeable anions [27–29]. Basic chemical formula of LDH is written as $[M_{1-x}{}^{z+}\ M_x{}^{3+}\ (OH)_2]^{y+}\ (X^{n-}{}_{y/n})\cdot mH_2O$, where z = 2; $M^{2+} = Mg^{2+}$, Zn^{2+}, Ni^{2+}, or Fe^{2+}; $M^{3+} = Al^{3+}$, Cr^{3+}, Mn^{3+}, or Fe^{3+}, and $X^{n-} = CO_3{}^{2-}$, $SO_4{}^{2-}$, F^-, Cl^-, $NO_3{}^-$ or OH^- [30,31]. So far, limited studies investigated LDH-contained dental sealants. Tammaro et al. [32], who adding the fluoride contained MgAl LDH to fissure sealant; results showed that low concentration of fluoride releasing from the LDH could promote the differentiation and proliferation of human dental pulp stem cells. However, fluoride recharging capacity, the release of leachable substances, discoloration of LDH-added resin composites and effects of LDH fillers in different particle sizes were not discussed.

In this study, the mechanical, physical, fluoride-releasing and rechargeable properties, and biocompatibility of a novel composite derived from commercial dental resin composites dispersed powder of LiAl LDH was investigated. The LiAl LDH intercalated with F- was prepared with different particle sizes, which contains monovalent (z = 1) and trivalent matrix cations as $[Li_{1-x}{}^+\ Al_x{}^+\ (OH)_2{}^{(2x-1)+}(A_{2x-1/n}{}^{n-})\cdot mH_2O$ [33,34]. Early studies have indicated that LiAl LDH exhibit an anion exchange capacity of ~4.8 (meq g^{-1}), which exceeds those of MgAl (~3.4 meq g^{-1}) and ZnAl (~3.0 meq g^{-1}) LDHs [35]. Beside, leaching of Al^{3+} and Li^+ will be measured in this work.

2. Experiments

2.1. *Preparation of the LiAl-F layered double hydroxide*

LiAl-CO_3 LDH (LDH-CO_3) was the raw material for preparing LiAl-F (LDH-F). The LDH-CO_3 LDH powder was synthesized by simply adding powdered AlLi intermetallic compound (IMC) to a stirred water-bath and followed processes reported in our previous study [36]. To have different particle sizes, the LDH-CO_3 was further ground either by wet ball milling (WLDH-CO_3) or dry ball milling (DLDH-CO_3) using a planetary ball mill (PM100, Retsch, Haan, Germany). The ball milling process was performed at a rotation speed of 400 rpm using zirconium dioxide (ZrO_2) vessels (125 ml) containing ZrO_2 ball (3 mm in diameter). Duration time was 30 min for one time, three times for dry ball milling, two times for wet ball milling (in alcohol). The milled powder was then processed by vacuum freeze-drying for 48 h. Brunauer–Emmett–Teller (BET) surface area was measured by high-resolution surface area and porosimetry analyzer (ASAP 2020, Micromeritics, Norcross, GA, USA). Microstructures were observed using a field-emission scanning electron microscope (SEM; JSM-6700F, JEOL, Tokyo, Japan).

The LDH-F was prepared by immersing 0.5 g LDH-CO_3 into the 200 ml aqueous containing 1000 ppm F- (prepared by NaF). The aqueous was magnetically stirred with argon bubbling (2 L/min) at room temperature for 40 min. The pH of the aqueous was adjusted at 6.0 ± 0.5 during immersing by dropwise addition of dilute nitric acid (5 vol. %). The errors in the fluo-

ride concentration caused by adding the nitric acid were lower than 5%. Finally, the powder in the aqueous was separated by centrifuge and was then processed by vacuum freeze-drying. To evaluate the absorption of fluoride in the LDH, fluoride concentrations (ppm) of the NaF aqueous were measured by Ion Chromatograph (ICS-900, DIONEX, Sunnyvale, CA, USA). In addition, to confirm the deintercalation of CO_3^{2-}, the concentration of escaped $CO_{2\,(g)}$ was recorded using a CO_2 detector (CPG 2000, JETEC, Taichung, Taiwan). The fluoridized powder (LDH-F) were analyzed by Fourier transform infrared spectrometer (FT-IR; Spectrum 65, Perkin Elmer, Waltham, MA, USA), each sample was mixed with oven-dried spectroscopic-grade KBr (1:100) and pressed into a disc with a diameter of 12.91 mm under around 8 tons of pressure for three minutes. The spectra of each sample were recorded by accumulating 100 scans at 1 cm^{-1} resolution between 400 and 4000 cm^{-1}. Crystallographic data were obtained using a glancing angle X-ray diffraction (GAXRD; MXP-III, MAC SCIENCE, Tokyo, Japan) with a Cu Kα radiation source. The diffraction patterns were collected from 6 to 60° in 2-theta at a rate of 3° per min.

2.2. Dispersion of the LDH-F into dental resin composites

A commercial light-activated resin composite (RX; Esthet-X Flow with shade A3, Densply, Milford, DE, USA) and a commercial compomer restorative material (CC; Dyract flow with shade A3, Densply, Milford, DE, USA) were used in this work (composition and labels were shown in Table 1).

The LDH-F powder (with a mass fraction of 3% and 5%) were dispersed into the resin composite and manually stirred for 3 min. The mixtures were then prepared as disks in triplicate with 6 mm in diameter and 2 mm thick in Teflon molds. Light curing with an irradiation time of 40 s for both sides was proceeded using a halogen light cure unit (CU-100 A, Rolence Enterprise, Taoyuan, Taiwan) which had an irradiance at 400–500 nm of about 380–450 mW/cm^2 (40 s for both sides). To understand the mechanical properties of the specimens under different light-curing radiant exposures, a high power multiwavelength light-emitting diode (LED) light cure (Valo Cordless, Ultradent Products, South Jordan, UT, USA) with a radiant exitance of 1400 mW/cm^2 light at 395–480 nm was employed (40 s for both sides).

2.3. Analysis technology and equipment

2.3.1. Determination of mechanical properties

The samples for mechanical tests were kept in the dry condition in a sealed centrifuge tube at room temperature (25–28 °C), keeping away from light. All the mechanical tests were completed within 3 days after the sample preparation. Knoop hardness tests were performed in quintuplicate by hardness tester (MXT70, Matsuzawa Seiki, Tokyo, Japan) at room temperature at a load of 500 g for a dwell time of 15 s. A smooth surface was obtained after sample demolding; the mean hardness value was then determined from the average of fifteen indents randomly selected on the sample surface. Flexural strength tests were conducted using an automatic testing stand (JSV-H1000, Japan Instrumentation System, Nara, Japan). Specimens with 25 ± 2 mm in length, 2 ± 0.1 mm in both width and height were prepared in quintuplicate for flexural strength testing at a test rate of 1 mm /1 min (flexural strength were tested to standard ISO 4049:1991).

2.3.2. Colorimetric analysis

Uniform Color Space (UCS) system developed by Commission Internationale de l'Eclairage (CIE) relating the color calculation to tristimulus values was used for the colorimetric analysis. Evaluation of movements in the white-black (L^* axis), red-green (a^* axis), and yellow-blue (b^* axis) were recorded in quintuplicate using a spectrophotometer (VITA Easyshade® Advance, Vita Zahnfabrik, Bad Säckingen, Germany). Changes in overall color ΔE^* were calculated as follows [37]: $\Delta E^* = ((L^*_2 - L^*_1)^2 + (a^*_2 - a^*_1)^2 + (b^*_2 - b^*_1)^2)^{1/2})$. In this work, L^*_1, a^*_1, b^*_1 correspond to the value in A3 shade of the porcelain shade guide (Lumin® Vacuum–Farbskala, Vita Zahnfabrik, Bad Säckingen, Germany) as a baseline, L^*_2, a^*_2, b^*_2 represent the measurements of each specimen.

2.3.3. Fluoride release assay

In the fluoride release assay, specimens were made in triplicate and the values of the measurements were averaged. The specimens were immersed and stored in centrifuge tubes with 3 ml deionized (DI) water individually at 37 °C. For the fluoride measurement, the specimens were removed from the centrifuge tubes and then placed to new centrifuge tubes with a fresh 3 ml DI water. The remaining solution was analyzed using fluoride ion selective electrode (Orion 9609 BNWP, Thermo Fisher Scientific, Waltham, MA, USA) after addition of a total ionic strength adjustor and a buffer solution (TISAB-III, Thermo Fisher Scientific, Waltham, MA, USA). The measurements were made each day and lasted for 90 days. Among the period, fluoride recharging was carried out during day 30–60 by immersing the specimens into 1000 ppm fluoride-containing solution for 4 min. After the immersion, the specimens were immediately washed for 1 min using DI water. The concentration of Al^{3+} and Li^+ by day 1, 7 and 30 were measured using inductively coupled plasma mass spectrometer (ICP-MS; 7500ce, Agilent, Agilent Technologies, Tokyo, Japan).

2.3.4. Cell cytotoxicity

The specimens were fabricated under a non-sterile condition. Some contaminants might also be generated while trimming the irregular edges of the specimens. In order not to influence the results of cytotoxicity tests, each specimen was ultrasonically cleaned in the DI water for 10 min and irradiated with ultraviolet light (UV) for 12 h to disinfect the surface. Each specimen was then individually immersed into a centrifuge tube with 6 ml α-minimum essential medium (α-MEM, supplemented with 10% horse serum and 1% PSA) and incubated at 37 °C for one day. For cell culture assay, Murine L929 fibrosarcoma cells at a concentration of 5×10^4 cells/well were directly seeded onto each specimen placed in 48-well plates and cultured with α-minimum essential medium (α-MEM) for one day and three days respectively (the α-MEM culture medium was renewed every two days). The results were normalized to a blank control group and compared to a positive control group (dimethyl sulfoxide, DMSO). Cytotoxic assays were conducted using a Cell Counting Kit-8 (CCK-8, Dojindo,

Table 1 – Materials used in this research.

Code	Materials	Type	Composition	Manufacturer
RX	Esthet-X Flow (shade A3)	Flowable composite	Bisphenol A glycidyl methacrylate (Bis-GMA), urethane modified Bis-GMA dimethacrylate, barium boron fluoro alumino silicate glass, polymerizable dimethacrylate resins and amorphous silica	DENTSPLY Caulk, Milford, DE, USA
R3			RX added 3% LDH-F	
R5			RX added 5% LDH-F	
R3W			RX added 3% WLDH-F	
R5W			RX added 5% WLDH-F	
R3D			RX added 3% DLDH-F	
R5D			RX added 5% DLDH-F	
CC	Dyract Flow (shade A3)	Flowable compomer	Strontium-alumino-fluoro-silicate glass, highly dispersed silicon dioxide, ammonium salt of PENTA (dipentaerythritol penta acrylate monophosphate) and N,N-dimethyl aminoethyl methacrylate, carboxylic acid modified methacrylate macromonomers, diethylene glycol dimethacrylate (DGDMA), camphorquinone, ethyl-4-dimethylaminobenzoate, 2-hydroxymethylbenzophenone, butylated hydroxyl toluene (BHT), and other stabilisers, Iron pigments, titanium dioxide	DENTSPLY Caulk, Milford, DE, USA

Kumamoto, Japan). The measurements were made in quintuplicate and the values were averaged.

2.4. *Statistical analysis*

The differences in Knoop hardness, flexural strength, color difference and cell cytotoxicity among the specimens were statistically analyzed with analysis of variance (ANOVA) followed by Tukey's post hoc tests (significance level 0.05).

3. Results and discussion

3.1. *Characterization of the LDH-CO3 with different particle sizes*

The microstructures of LDH-CO_3, WLDH-CO_3, and DLDH-CO_3 were illustrated in supplementary information Fig. S1. The BET surface areas data for the three LDH powder samples were obtained. As a result, the specific surface area of the LDH-CO_3 was around 9.64 (m^2/g). For comparison, the WLDH-CO_3 had specific surface areas of 14.87 (m^2/g), and the DLDH-CO_3 had 54.54 (m^2/g). These results demonstrated that the specific surface area of LDH was raised after ball milling. Among wet and dry ball milling process, the later effectively raised its BET surface area from 9.64 (m^2/g) to 54.54 (m^2/g).

3.2. *Analysis of the LDH-F*

The LDH-F powders were prepared by immersion of fluoride-containing solution. The processing parameters for fabricating the LDH-F were described in the supplementary information

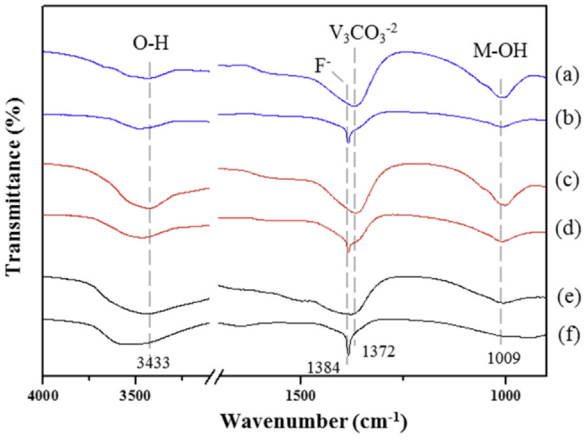

Fig. 1 – FT-IR spectra of LDH-CO_3 (a), LDH-F (b), WLDH-CO_3 (c), WLDH-F (d), DLDH-CO_3 (e) and DLDH-F (f).

of Fig. S2. The LDH-F powders were characterized by FT-IR spectroscopy and X-ray diffraction. The XRD patterns of the fluoridized LDHs were illustrated in Fig. S3. Spectra of FT-IR were shown in the Fig. 1. In high-frequency region, the spectrum shows broad bands at 3433 cm^{-1} attributed to the hydroxyl-stretching mode, caused by hydroxyl groups and the interlayered water molecules of the LDH. The absorption band around 1372 cm^{-1} is corresponding to the vibrational absorption of the interlayered CO_3^{2-}. After the fluoridization process, the strong and sharp peak was found at 1384 cm^{-1} which represented the intercalation of fluoride [38,39]. Moreover, the board band at 3433 cm^{-1} was a shift to a higher frequency

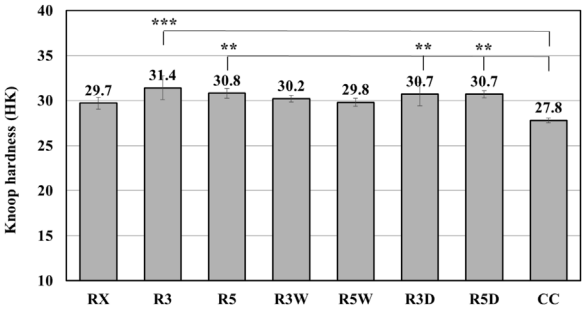

Fig. 2 – The Knoop hardness test at room temperature. (Significant difference: *P < 0.05; **P < 0.01; ***P < 0.005).

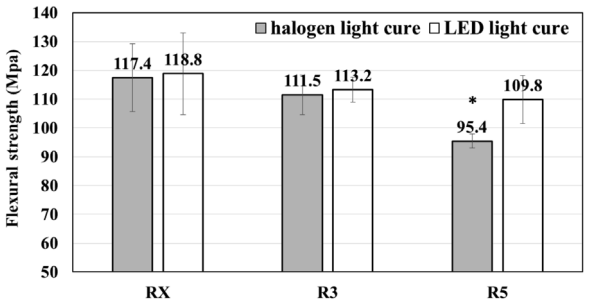

Fig. 4 – The flexural strength test. The samples were cured with either halogen light cure or LED light cure. The test was performed at a test rate of 1 mm /1 min at room temperature. (*: significant difference to RX group).

around 3508 cm^{-1} after fluoride absorption, which corroborated the interaction of intercalated fluoride with hydroxyl groups [40].

3.3. *Combination of the LiAl-F LDH with dental resin composites*

3.3.1. *Determination of mechanical properties*

Results of Knoop hardness tests are shown in the Fig. 2. The results of the ANOVA show statistically differences among groups (F (7, 23) = 4.64; p = 0.00527). The resin composites possess higher hardness compared to other types of dental restorations: compomer, conventional GIC or resin-modified GIC [41]. Although the LDH-contained specimens presented no significant difference to the RX shown by Tukey test, mean surface hardness of R3 (31.4 HK), R5 (30.8 HK), R3W (30.2 HK), R5W (29.8 HK), R3D (30.7 HK) and R5D (30.7 HK) were slightly higher than the RX (29.7 HK). Moreover, the microhardness of LDH-contained resin composites (R3, R5, R3D, and R5D) was significantly higher than that of the compomer (CC). It could be speculated that the morphology of the rosette-shapes LDH might increase a distance of crack-extension and result in the higher surface hardness. Besides, the nanoparticles have been known for dispersion hardening, which could be the reason for the increased hardness [42,43].

The results of the flexural strength test are shown in the Fig. 3. The ANOVA analysis reveal that significant differences among groups [F (7, 24) = 4.69164; p = 0.00435]. The compomer group (CC) presented the lowest strength in comparison to the other resin composite groups in line with the results of

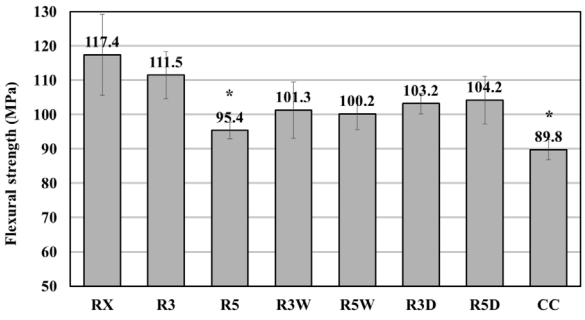

Fig. 3 – The flexural strength test. The test was performed at a test rate of 1 mm /1 min at room temperature. (*: significant difference to RX group).

previous studies [20]. Post hoc comparison indicated that the R5 exhibited a significant lower strength than the other LDH-contained specimens. The variations in the flexural strength of the resin composites can be influenced by the following factors: (1) attenuated curing light exposure, and (2) dispersive strengthen of filler materials.

LiAl LDH has been known as a nearly opaque material, which has been reported the maximum transmittance of 9.4% in the visible region and less than 1% in the short wavelength region (λ < 500 nm) at 28 °C) [44]. However, the resin composite in this work contains camphorquinone (CQ), a typical visible light-activated photoinitiator that initiates polymerization in an absorbance range between 400 and 500 nm (max = 470 nm) [45]. It means that the strength of the LDH-contained resin composite should be susceptible to the output power of the curing light. There could be a light shielding effect resulting in a low degree of crosslinking in the LDH-contained resin composites. Moreover, Rueggeberg et al. [46] have shown that the light irradiances should be above 233 mW/cm^2 to provide adequate energy for a sufficient cure of composite layers of 1 mm thickness. In this research, even the light curing was performed on both sides of the specimens (a thickness of 2 ± 0.1 mm), the irradiance of the halogen light (380–450 mW/cm^2) would attenuate under the "light shielding effect" and the irradiance may become lower than the critical value reported (233 mW/cm^2). Therefore, to verify the hypothesis of the "shielding effect" by the LDH additives, pre-preparation of RX, R3, and R5 was done and cured with 1400 mW/cm^2 LED light cure for both sides. The RX samples (cured with the halogen light cure and the LED light cure) show similar flexure strength (Fig. 4), which means the flexural strength was not changed remarkably under fully cured with a strong LED light source. However, as expected, a higher flexural strength was found in the LED-cured R5 than in the halogen light cured R5, which confirmed the hypothesis of shielding effect caused by the rosette-shaped LDH.

Nano-size fillers have been extensively used as reinforcing fillers in composites. However, R3D or R5D presented unobvious reinforcement. It can be speculated that inorganic fillers or pigments are already present in the resin composite (61% filler by weight, 53% by volume) designed by the manufacturer, which have given a sufficient reinforcement to matrices. Hence, reinforcement of the nano-size LDH filler was dif-

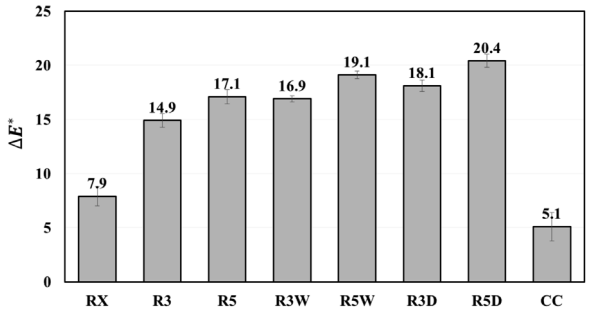

Fig. 5 – The color difference ΔE* between vita A3 shade guide and each samples. (n = 5).

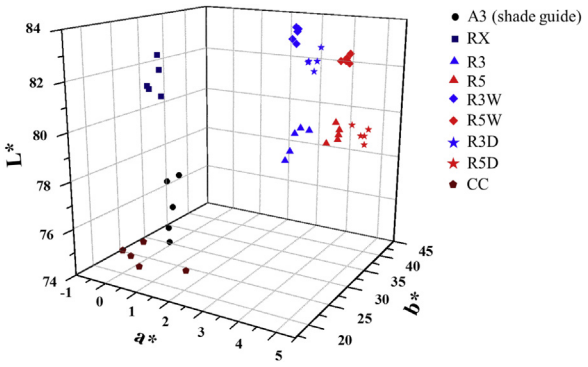

Fig. 6 – Color spatial plot (CIE L*a*b*) of RX, RX with LDH, and CC comparing to the Vita A3 shade guide. (n = 5).

ficult to be distinguished unless reducing amounts of the pre-existed fillers or the pigments. As the results, a better mechanical reinforcement could be achieved by the rosette-shaped LDH particles compared to those with the ball milling treatment.

Another possible explanation to why the composite resin did not be further strengthened by the nano-sized LDH is that the manual agitation would cause few bubbles, which can be found on the fracture surface of the LDH contained resin specimen by SEM observation. Nevertheless, the flexural strength of the RX resin with nano-sized LDH is not inferior to the control RX resin. Herein, one cannot ignore the possible effect of the existing bubbles leading to the deterioration of the mechanical properties. This result suggests that there is still a need for optimizing the preparation technique for the LDH contained resin sample. Especially, when scale-up the fabricating process for commercializing production is required in the future, a mechanical mixer under vacuum should be employed to remove these bubbles effectively, and higher strength can be expected.

The dental composite is considered to be used for over 7 years (with a survival rate of 67.4%) in permanent teeth [47]; therefore, additional studies would be needed to clarify the effect of LDH on the properties such as the long term stability, wear resistance and mechanical properties after thermal cycle.

3.3.2. *Colorimetric analysis*

Results of the colorimetric analysis were shown in the Fig. 6. The CIE $L^*a^*b^*$ system [37] uses the three parameters L^*, a^*, and b^* to define color. L^* corresponds to the degree of lightness and darkness, while $+a^*$ and $-a^*$ correspond to red and green, $+b^*$ and $-b^*$ correspond to yellow and blue. Several reports have shown that changes in overall color (ΔE^*) in the range of 2–3 were just perceptible [48,49] and the critical value for visual perception was 3.3. On this basis, all the specimens in this study had perceptible color changes shown as Fig. 5. According to recent statistics by Elamin et al. [50], A3 was the most common tooth shade in 227 patients across an extensive age range from 15 to 72 years. Although RX ($\Delta E^* = 7.9$) and CC (5.1) are in the A3 shade claimed by manufacturers, perceptible color changes were observed comparing to the porcelain shade guide. Several reports have indicated that only a few restorative materials gave an excellent color match even though they were claimed by their manufacturers to match the Vita shade guide [51,52]. Besides, the results revealed that the ΔE^* had a significant positive linear correlation with the amounts of the LDH contained. Among them, the mean ΔE^* of the R3 (14.9) and the R5 (17.1) were lower than the R3W (16.9), the R5W (19.1), the R3D (18.1), the R5D (20.4). This fact indicated that the rosette-shaped LDH could give a lower discoloration compared to those treated with the ball milling treatment.

For the LDH-contained resin composites (shown as Fig. 6), there is no significant change in L^* but a slight rise in a^* and obvious increases in b^* with increasing amounts of the LDH. The fact could be explained by the optical properties of the LiAl LDH reported by our previous study [44]. The absorbance spectra revealed that light absorbance was inversely proportional to the wavelength in the visible region, which means that the absorbance in the green region (495–570 nm) were higher than the red region (620–750 nm) and caused a rise in the a^*. Likewise, the absorbance in the blue region (476–495 nm) was higher than the yellow region (570–590 nm) and caused a rise in the b^*. Besides, the transmittance spectra of LiAl LDH by our previous study [44] indicated that the transmittance became higher around the red region, which implied that a fraction of light in the red region penetrated and lowered the extent of rise in the a^*. As the results, containing 3% or 5% LiAl LDH could cause slight rises of the a^* (redder) and obvious rises of the b^* (more yellow) in chromatics for the resin composite. According to statistics by Elamin et al., there was a significant relationship between age and CIE $L^*a^*b^*$ coordinates; teeth become darker, yellower and redder with an increase of age [50]. The color appearance of LDH can be adjusted by altering the divalent metal cations within their structure. For example, LDHs containing Li^+, Mg^{2+}, Ca^{2+}, Al^{3+} present a white appearance, where Fe^{3+} contained LDH presents yellow or red-to-brown color. Therefore the color matching of dental composites toward the tooth color shades can be achieved by doping with different kinds of F-LDH instead of using other pigments. The fact indicated that the LDH was given a color adjustment potential in clinical application.

3.3.3. *Fluoride-releasing and rechargeability*

Results of fluoride measurement are presented in the Fig. 7. To investigate the fluoride release and fluoride recharge properties of the LDH-contained resin composites, the fluoride measurement was divided into three periods: (i) fluoride

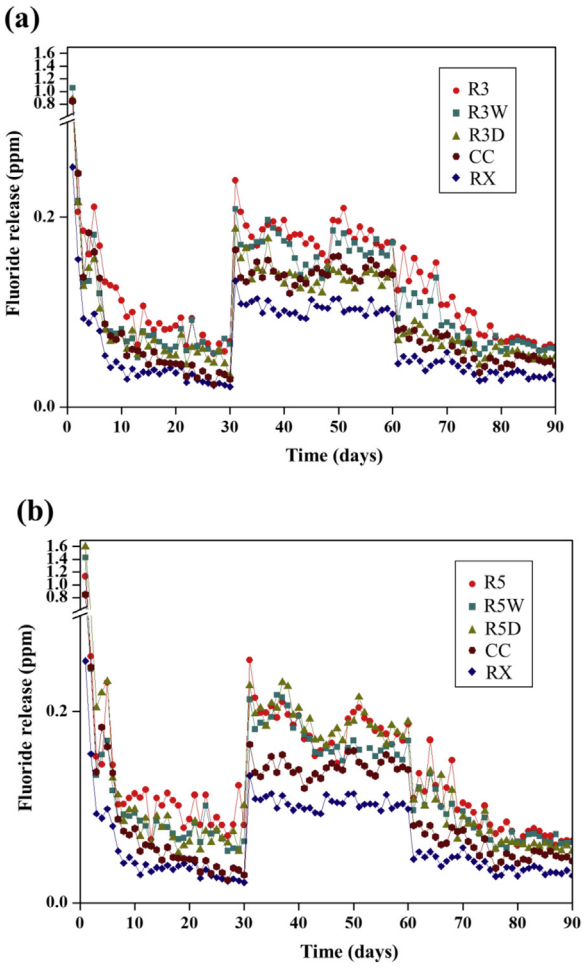

Fig. 7 – The daily fluoride releasing profile of (a) RX with 3% LDH, CC, and RX, (b) RX with 5% LDH, CC, and RX, The measurements were performed in three periods: (i) initial fluoride release (1-30 days), (ii) fluoride recharge (31–60 days), and (iii) fluoride release after recharge for 30 days (61–90 days). (For interpretation of the references to color in the text, the reader is referred to the web version of this article.).

release (1–30 days), (ii) fluoride recharge and release (31–60 days) and (iii) fluoride release (61–90 days).

In the first period, fluoride burst behavior was observed at the beginning of the experiment: RX (0.25 ppm), R3 (0.86 ppm), R5 (1.13 ppm), R3W (1.06 ppm), R5W (1.43 ppm), R3D (0.87 ppm), R5D (1.60 ppm) and CC (0.85 ppm). Among them, a low amount of fluoride releasing was found in the RX, which was attributed to a small amount of fluoride salts existed in the as-received RX (the composition from the manufacturer was shown in Table 1). Burst behavior has been known as a general phenomenon which often involved a quick release of the substance from the substrate at the surface of a material in the earlier stage [32,53]. In the following weeks, the fluoride release leveled off obviously for each specimen. It has been reported that two elution processes of fluoride release, one short-term release occurred from the surface of a material in the earlier stage, the other long-term release which mainly comes from the inner part of the material exhibiting slower or prolonged release [54]. It's reasonable to expect that containing of ball-milled LDH fillers presented a higher and rapid fluoride release than the rosette-shape one in earlier stage due to the higher specific surface area. The rosette-shaped LDH fillers presented an unobvious fluoride burst in the earlier stage but prolonged fluoride release in the following days, indicating the better stability of fluoride release. Besides, the commercial compomer was found a rapid fluoride release in an earlier stage, followed by an obvious decrease toward a value approximated to the RX, which showed poor stability in fluoride release than that of each of the LDH-contained specimen. It has been reported that significant inhibition of proliferation on the human dental pulp stem cells (hDPSC) was observed while the concentration of fluoride raised to 3 or 5 ppm [32], the value was not presented in each specimen in this study. Additionally, an inverse phenomenon of fluoride release were observed during day 2 to day 4, which might be caused by a new diffusive mechanism forming a new diffusive path after water absorption in resin composites.

In the second period, the fluoride recharge was carried out each day. For all the specimens, the fluoride release was increased after fluoride recharge. Among them, the RX showed a fluoride recharge capacity with a raise of fluoride release from $\tilde{0}$.02 ppm to $\tilde{0}$.1 ppm. Those containing the 5% LDH showed a rise of fluoride release from $\tilde{0}$.07 ppm to $\tilde{0}$.2 ppm, the increasing amounts of fluoride releasing were higher than the RX. Besides, the CC presented a raise of fluoride release from $\tilde{0}$.03 ppm to $\tilde{0}$.14 ppm. The rechargeability of resin composites is thought to depend on the absorption and diffusion effects by the presence of porosity within the matrix [55]. A low recharge capability was observed in the RX, but an obvious rise was found in those LDH-contained resin composites. Even the CC consisted of several glass ionomers, the recharging capability still lower than the 5% LDH-contained resin composites. Previous studies suggested the mechanism of fluoride recharge on clay filler was based on adsorption of fluoride [56]. In this work, there may be an additional mechanism of fluoride recharge based on the ion exchanging in the interlayer's space in the LDH. Therefore the composites containing LDH fillers showed a superior recharging capability.

Termination of fluoride recharge in the third period, a rapid declination of fluoride release was observed in the CC and the RX while the LDH-contained resin composites presented a slower decrease and prolonged to release the fluoride. In general, most of the compomers containing pre-reacted glass can serve as a fluoride reservoir and have a higher fluoride release amount and recharge capabilities [55]. In this study, the RX showed lower fluoride release than the CC, while most LDH-contained resin composites exhibited an optimization in fluoride recharge capacity and had a higher fluoride release than the CC. It has been reported that remineralization was enhanced at levels of 0.03 ppm fluoride and an optimum being achieved at about 0.08 ppm or higher in the calcium phosphate mineralization solution [25]. Although exhibiting a smaller amount of fluoride released comparing to those glass-ionomer cement (GICs) reported, the LDH-contained resin composite provides a sufficient level of fluoride for enhancing remineralization.

3.3.4. *Leaching of Al3+ and Li+ ions*

The release of Al^{3+} and Li^{+} ions from RX, R5, R5D, and CC were shown in the Fig. 8. In the first day, a low amount of concentration (ppm) of Al^{3+} was measured in each specimen. By day 7 and 30, all the specimens exhibited a rapid decline to a very low concentration of Al^{3+}. It has been demonstrated that the considerable release of Al^{3+} caused several well-known toxic effects in humans, including adverse effects on the central nervous system, skeleton and a possible contributing factor in the development of Alzheimer's disease [57]. Early studies by Andersson and Dahl [21] showed that the Al^{3+} released from some commercial glass ionomer cement was up to hundreds of ppm during earlier water exposure in vitro, which may lead to adverse effects on humans. Although the LiAl LDH contained 23.88–25.28 wt% Al reported in former studies [36], only a small amount of Al^{3+} was measured during water exposure. The result indicates that the addition of LiAl LDH in a proportion of 5 wt% didn't cause large amounts of Al^{3+} to be released. On the other hand, a very low amount of Li^{+} (ppb) was measured. Li^{+} has been known for enhancing or preserving bone mass due to increased proliferation rates and alkaline phosphatase activity of osteoblastic cells [58,59]. Besides, in a recent study, the Li^{+} has suggested the enhancements of the proliferation, differentiation and cementogenic

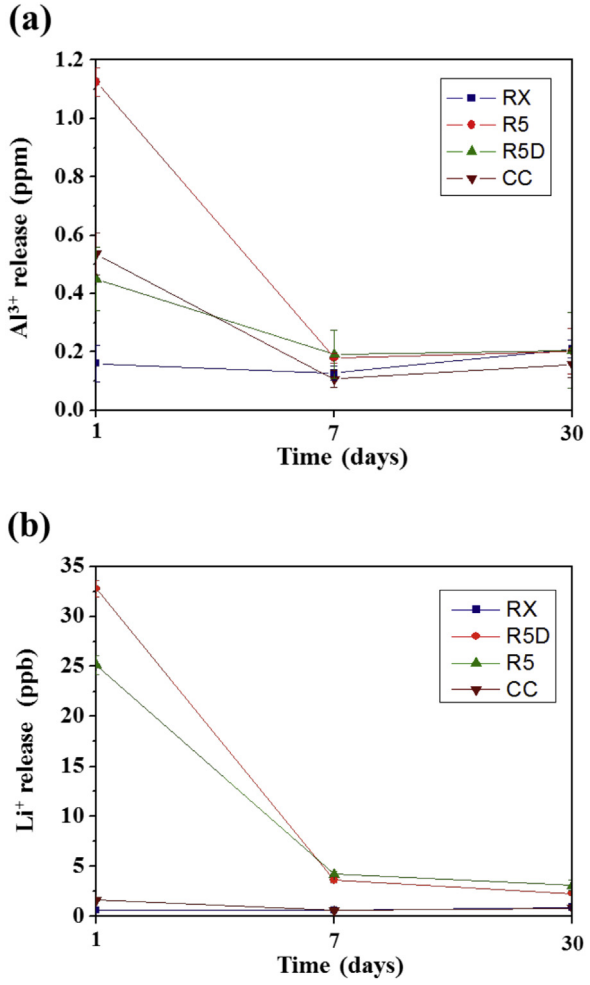

Fig. 8 – The associated Al3+ and Li+ ions release after 1, 3, and 7 days immersion in de-ionized water.

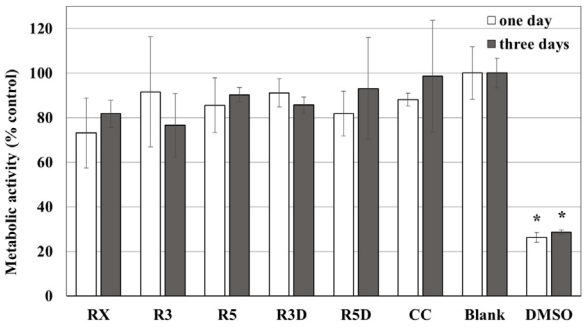

Fig. 9 – Cytotoxic effects of each specimen on L929 cells after 1 and 3 days of culture. (*: significant difference to other groups).

gene expression of PDLCs [21]. Although Li^{+} releasing from R5 and R5D were significantly lower than which designed for bioactive functions mentioned above, which provides the possible benefits to human.

3.3.5. *Cell cytotoxicity*

The cell viability of each specimen after culture for one day and three days are presented in the Fig. 9. The results of the ANOVA show that there are statistically significant differences ($F(7, 22) = 4.64$; $p = 2.01131E\text{-}4$). Although there were no significant differences between each specimen analyzed by the Tukey test, the LDH-contained resin composites present slightly higher cell viability than the RX. There have been reported that cytotoxicity existed in some resin-based composites due to the release of free monomers or leachable substance [60,61]. However, LDH-contained resin composite did not show any lower cell viability but a slight rise compared to the RX. Thus it can be concluded that there was no potential cytotoxicity in each specimen with a value of cell viability higher than 70% defined by ISO10993-5.

4. Conclusions

It can be concluded that the addition of the LDH filler significantly improved the fluoride release of dental resins composites in this research. An optimization in the fluoride release and the fluoride recharge capability are found in the LDH-contained resin composites. Besides, different fluoride releasing properties are observed in different particle sizes of the LDH fillers. The R5W and the R5D with smaller particle sizes were given a higher and rapid fluoride release in an early stage due to the high surface area. In the other hand, the R5 with rosette-shaped LDH particles showed a low amount of fluoride in the earlier stage but prolonged the fluoride release. In this study, the results of fluoride release, mechanical properties, color change, ion leaching and cytotoxicity of the LDH-contained resin composites showed the LDH a potential material as filler for the dental resins.

Acknowledgments

The authors would like to thank the Ministry of Science and Technology, Taiwan, R.O.C. (MOST 105-2314-B-039-046-MY2,

MOST 104-2221-E-005-013-MY3, and MOST 107-3113-E-006-010-) for supporting this research. Moreover, the study was also supported in part by the Ministry of Education, Taiwan, R.O.C. under the Higher Education Sprout Project for funding this project.

Appendix A. Supplementary data

Supplementary data associated with this article can be found, in the online version, at https://doi.org/10.1016/j.dental.2019.02.002.

REFERENCES

[1] Petersen PE, Lennon MA. Effective use of fluorides for the prevention of dental caries in the 21st century: the WHO approach. Community Dent Oral Epidemiol 2004;32:319–21.
[2] Kaste LM, Selwitz RH, Oldakowski RJ, Brunelle JA, Winn DM, Brown LJ. Coronal caries in the primary and permanent dentition of children and adolescents 1–17 years of age: United States, 1988–1991. J Dent Res 1996;75:631–41.
[3] Buonocore MG. A simple method of increasing the adhesion of acrylic filling materials to enamel surfaces. J Dent Res 1955;34:849–53.
[4] Newbrun E. Effectiveness of water fluoridation. J Public Health Dent 1989;49:279–89.
[5] Twetman S, Axelsson S, Dahlgren H, Holm AK, Källestål C, Lagerlöf F, et al. Caries-preventive effect of fluoride toothpaste: a systematic review. Acta Odontol Scand 2009;61:347–55.
[6] Horowitz HS, Creighton WE, McClendon BJ. The effect on human dental caries of weekly oral rinsing with a sodium fluoride mouthwash: a final report. Arch Oral Biol 1971;16:609–16.
[7] Weisz WS. The reduction of dental caries through use of a sodium fluoride mouthwash. J Am Dent Assoc 1960;60:438–56.
[8] Featherstone JD, Glena R, Shariati M, Shields CP. Dependence of in vitro demineralization of apatite and remineralization of dental enamel on fluoride concentration. J Dent Res 1990;69:620–5.
[9] Hamilton IR. Biochemical effects of fluoride on oral bacteria. J Dent Res 1990;69:660–7.
[10] Marquis RE. Antimicrobial actions of fluoride for oral bacteria. Can J Microbiol 1995;41:955–64.
[11] ten Cate JM, Duijsters PP. Influence of fluoride in solution on tooth demineralization. Caries Res 1983;17:193–9.
[12] ten Cate JM, Featherstone JD. Mechanistic aspects of the interactions between fluoride and dental enamel. Crit Rev Oral Biol Med 1991;2:283–96.
[13] Lee H, Ocumpaugh DE, Swartz ML. Sealing of developmental pits and fissures: II. Fluoride release from flexible fissure sealers. J Dent Res 1972;51:183–90.
[14] el-Mehdawi SM, Rapp R, Draus FJ, Miklos FL, Zullo TG. Fluoride ion release from ultraviolet light-cured sealants containing sodium fluoride. Pediatr Dent 1985;7:287.
[15] Wilson AD, Kent BE. The glass-ionomer cement, a new translucent dental filling material. J Chem Technol Biotechnol 1971;21:313.
[16] Neelakantan P, John S, Anand S, Sureshbabu N, Subbarao C. Fluoride release from a new glass-ionomer cement. Oper Dent 2011;36:80–5.
[17] Simonsen RJ. Glass ionomer as fissure sealant—a critical review. J Public Health Dent 1996;56:146–9.
[18] Smith DC. Development of glass-ionomer cement systems. Biomaterials 1998;19:467–78.
[19] Sidhu SK, Sherriff M, Watson TE. The effects of maturity and dehydration shrinkage on resin-modified glass-ionomer restorations. J Dent Res 1997;76:1495–501.
[20] Janda R, Roulet JF, Latta M, Rüttermann S. The effects of thermocycling on the flexural strength and flexural modulus of modern resin-based filling materials. Dent Mater 2006;22:1103–8.
[21] Andersson ÖH, Dahl JE. Aluminium release from glass ionomer cements during early water exposure in vitro. Biomaterials 1994;15:882–8.
[22] Bapna MS, Mueller HJ. Leaching from glass ionomer cements. J Oral Rehabil 1994;21:577–83.
[23] Savarino L, Cervellati M, Stea S, Cavedagna D, Donati ME, Pizzoferrato A, et al. In vitro investigation of aluminum and fluoride release from compomers, conventional and resin-modified glass-ionomer cements: a standardized approach. J Biomater Sci Polym Ed 2000;11:289–300.
[24] Itota T, Carrick TE, Rusby S, Al-Naimi OT, Yoshiyama M, McCabe JF. Determination of fluoride ions released from resin-based dental materials using ion-selective electrode and ion chromatograph. J Dent 2004;32:117–22.
[25] Featherstone JD. Prevention and reversal of dental caries: role of low level fluoride. Community Dent Oral Epidemiol 1991;27:31–40.
[26] O'reilly MM, Featherstone JD. Demineralization and remineralization around orthodontic appliances: an in vivo study. Am J Orthod Dentofacial Orthop 1987;92:33–40.
[27] Wang Q, O'Hare D. Recent advances in the synthesis and application of layered double hydroxide (LDH) nanosheets. Chem Rev 2012;112:4124–55.
[28] Rocha MA, Petersen PAD, Teixeira-Neto E, Petrilli HM, Leroux F, Taviot-Gueho C, et al. Layered double hydroxide and sulindac coiled and scrolled nanoassemblies for storage and drug release. RSC Adv 2016;6:16419–36.
[29] Rouahna N, Barkat D, Ouakouak A, Srasra E. Preparation of Mg–Al layered double hydroxide adsorbent: characterization and adsorptive removal of Co (II) ions from aqueous solutions. Sens Lett 2017;15:655–62.
[30] Manzi-Nshuti C, Wang D, Hossenlopp JM, Wilkie CA. The role of the trivalent metal in an LDH: synthesis, characterization and fire properties of thermally stable PMMA/LDH systems. Polym Degrad Stabil 2009;94:705–11.
[31] Inayat A, Klumpp M, Schwieger W. The urea method for the direct synthesis of ZnAl layered double hydroxides with nitrate as the interlayer anion. Appl Clay Sci 2011;51:452–9.
[32] Tammaro L, Vittoria V, Calarco A, Petillo O, Riccitiello F, Peluso G. Effect of layered double hydroxide intercalated with fluoride ions on the physical, biological and release properties of a dental composite resin. J Dent 2014;42:60–7.
[33] Besserguenev AV, Fogg AM, Francis RJ, Price SJ, O'Hare D. Synthesis and structure of the gibbsite intercalation compounds [LiAl2 (OH) 6] X {X= Cl, Br, NO3} and [LiAl2 (OH) 6] Cl•H2O using synchrotron x-ray and neutron powder diffraction. Chem Mater 1997;9:241–7.
[34] Serna CJ, Rendon JL, Iglesias JE. Crystal-chemical study of layered [Al2Li(OH6)+X-nH2O] [double hydroxide, hydrocalcite, lithium]. Clay Clay Min 1982;30:180–4.
[35] Leroux F, Besse JP. Polymer interleaved layered double hydroxide: a new emerging class of nanocomposites. Chem Mater 2001;13:3507–15.
[36] Lin MC, Chang FT, Uan JY. Synthesis of Li–Al-carbonate layered double hydroxide in a metal salt-free system. J Mater Chem 2010;20:6524–30.
[37] Robertson AR. The CIE 1976 color-difference formulae. Color Res Appl 1977;2:7–11.

[38] Lv L, He J, Wei M, Evans DG, Duan X. Factors influencing the removal of fluoride from aqueous solution by calcined Mg–Al–CO3 layered double hydroxides. J Hazard Mater 2006;133:119–28.
[39] Ma W, Zhao N, Yang G, Tian L, Wang R. Removal of fluoride ions from aqueous solution by the calcination product of Mg–Al–Fe hydrotalcite-like compound. Desalination 2011;268:20–6.
[40] Liu H, Deng S, Li Z, Yu G, Huang J. Preparation of Al–Ce hybrid adsorbent and its application for defluoridation of drinking water. J Hazard Mater 2010;179:424–30.
[41] Peutzfeldt A, García-Godoy F, Asmussen E. Surface hardness and wear of glass ionomers and compomers. Am J Dent 1997;10:15–7.
[42] Xia Y, Zhang F, Xie H, Gu N. Nanoparticle-reinforced resin-based dental composites. J Dent 2008;36(6):450–5.
[43] Zhao J, Xie D. Effect of nanoparticles on wear resistance and surface hardness of a dental glass-ionomer cement. J Compos Mater 2009;43(23):2739–52.
[44] Hsieh ZL, Lin MC, Uan JY. Rapid direct growth of Li–Al layered double hydroxide (LDH) film on glass, silicon wafer and carbon cloth and characterization of LDH film on substrates. J Mater Chem 2011;21:1880–9.
[45] Ogunyinka A, Palin WM, Shortall AC, Marquis PM. Photoinitiation chemistry affects light transmission and degree of conversion of curing experimental dental resin composites. Dent Mater 2007;23:807–13.
[46] Rueggeberg FA, Caughman WF, Curtis Jr JW, Davis HC. Factors affecting cure at depths within light-activated resin composites. Am J Dent 1993;6:91–5.
[47] Bernardo M, Luis H, Martin MD, Leroux BG, Rue T, Leitao J, et al. Survival and reasons for failure of amalgam versus composite posterior restorations placed in a randomized clinical trial. J Am Dent Assoc 2007;138(6):775–83.
[48] Doray PG, Wang X, Powers JM, Burgess JO. Accelerated aging affects color stability of provisional restorative materials. J Prosthodont 1997;6:183–8.
[49] Ruyter IE, Nilner K, Möller B. Color stability of dental composite resin materials for crown and bridge veneers. Dent Mater 1987;3:246–51.
[50] Elamin HO, Abubakr NH, Ibrahim YE. Identifying the tooth shade in group of patients using vita easyshade. Eur J Dent 2015;9:213–7.
[51] Seghi RR, Gritz MD, Kim J. Colorimetric changes in composites resulting from visible-light-initiated polymerization. Dent Mater 1990;6:133–7.
[52] Yap AU, Bhole S, Tan KB. Shade match of tooth-colored restorative materials based on a commercial shade guide. Quintessence Int 1995;26:697–702.
[53] Zhao J, Platt JA, Xie D. Characterization of a novel light-cured star-shape poly (acrylic acid) composed glass-ionomer cement: fluoride release, water sorption, shrinkage, and hygroscopic expansion. Eur J Oral Sci 2009;117:755–65.
[54] Tay WM, Braden M. Fluoride ion diffusion from polyalkenoate (glass-ionomer) cements. Biomaterials 1998;9:454–6.
[55] Xu X, Burgess JO. Compressive strength, fluoride release and recharge of fluoride-releasing materials. Biomaterials 2003;24:2451–61.
[56] Wang YL, Lee BS, Chang KC, Chiu HC, Lin FH, Lin CP. Characterization, fluoride release and recharge properties of polymer–kaolinite nanocomposite resins. Compos Sci Technol 2007;67:3409–16.
[57] Yokel RA, McNamara PJ. Aluminium toxicokinetics: an updated minireview. Basic Clin Pharmacol Toxicol 2001;88:159–67.
[58] Khorami M, Hesaraki S, Behnamghader A, Nazarian H, Shahrabi S. In vitro bioactivity and biocompatibility of lithium substituted 45S5 bioglass. Mater Sci Eng C-Mater Biol Appl 2011;31:1584–92.
[59] Zamani A, Omrani GR, Nasab MM. Lithium's effect on bone mineral density. Bone 2009;44:331–4.
[60] Goldberg M. In vitro and in vivo studies on the toxicity of dental resin components: a review. Clin. Oral Investig 2008;12:1–8.
[61] Schweikl H, Spagnuolo G, Schmalz G. Genetic and cellular toxicology of dental resin monomers. J Dent Res 2006;85:870–7.